Check for updates

Received: 21 July 2023 | Revised: 8 September 2023 | Accepted: 13 September 2023

DOI: 10.1111/jace.19472

Journal of the American Ceramic Society

RESEARCH ARTICLE

Assessment of structural and thermoluminescence characteristics of porcelain used as an electrical insulator

Ziyafer Gizem Portakal-Uçar | **Sibel Akça-Özalp** | **Mehmet Oglakci** | **Aya Barad** | **Mustafa Topaksu**

Department of Physics, Faculty of Arts-Sciences, University of Cukurova, Adana, Turkey

Correspondence
Ziyafer Gizem Portakal-Uçar, Department of Physics, Faculty of Arts-Sciences, University of Cukurova, Adana 01330, Turkey.
Email: gportakal@cu.edu.tr, gizemsry@gmail.com

Funding information
Research Fund of Cukurova University, Turkey, Grant/Award Number: FBA-2021-14293

Abstract

In the present work, the thermoluminescence (TL) properties and kinetics of beta-irradiated porcelain used as an electrical insulator are investigated in great depth. Thermal annealing at 1100°C slightly changes the trap system, whereas heating over 500°C increases the visual TL intensity of the peaks. X-ray diffraction, scanning electron microscopy with energy dispersive X-ray spectroscopy, atomic absorption spectroscopy, and Fourier transform infrared spectroscopy were used to confirm the structural, morphological, and chemical investigations of the materials. The TL glow curve characteristics, repeatability, storage time properties, and dose–response behavior of non-annealed and annealed porcelain have all been well investigated. Within the confidence interval, the material has been demonstrated to have excellent reusability. A linear response in the dose range of 0.1–3 Gy was observed. T_M–T_s, initial rise, and computerized glow curve deconvolution methodologies were used to complete the kinetic study. The outcomes of the detailed investigations demonstrated that the sample was suitable for TL dosimetry potential uses.

KEYWORDS
annealing, CGCD, porcelain, thermoluminescence, XRD

1 | INTRODUCTION

To research the effects of radiation, thermoluminescence (TL) is a fundamental application technique in radiation dosimetry. Its primary use is in calculating the absorbed dose caused by radiation events, in addition to background radiation as usual. According to the underlying TL theory, when an object is excited by ionizing radiation, the accumulated radiation energy is stored in the crystal lattice. When the crystal is heated, the stored radiation energy is immediately converted into photo-energy and released as TL, a type of phosphorescence. The TL mechanism is based on the electron transition from the ground state to an excited level in insulators or semiconductors.[1] For this purpose, various natural and synthetic materials are widely studied in TL dosimetry studies. Particularly, easily accessible materials are crucial for studying radiation impacts since they are simple to obtain and evaluate when needed. One such material is the ceramic insulators, which are utilized on high-voltage electrical supply lines. The porcelain used in the production of these insulators is electro-technical porcelain. This is made of quartz and field spat, which is a feldspar glass phase loaded with silicon oxide with a fine crystallite quartz phase distributed throughout. Some types of electro-technical ceramic are prepared using kaolin, which is an aluminum-rich silicate ($Al_2Si_2O_5(OH)_4$).[2] Good insulating porcelains are frequently used in parts such as ordinary switches, fuses and sockets, especially in old-style buildings. For more than 150 years, porcelain has been utilized as an electrical

 © 2023 The American Ceramic Society.

insulating medium. It has been realized over a long period of time that some characteristics of porcelain as a ceramic product, such as mechanical strength, high-power dielectric strength, and corrosion resistance, cannot be replicated in other materials.[3]

In general, different morphological, structural, and functional characteristics are required when a novel luminous material is suggested as a candidate for radiation applications. Detailed analyses are carried out independently when the samples are brought to the proper size. X-ray diffraction (XRD), scanning electron microscopy with energy dispersive X-ray spectroscopy (SEM-EDS), and atomic absorption spectroscopy (AAS) are methods that can be used to detect the phase composition, surface morphology, and trace element concentrations. Furthermore, Fourier transform infrared spectroscopy (FTIR) is used to determine and quantify the structure of a compound by examining the infrared that is absorbed through a sample's molecules and then converted to the interatomic vibrational energy of the atoms that make up the molecules, either in the form of stretching or bending.[4] The two most common forms of porcelain insulators are made of silica and alumina. In silica porcelain, high firing temperatures or extended firing times cause the quartz grains to melt, reducing the amount of solid quartz in the ceramic body. Aluminum oxide replaces quartz in large quantities in the alumina porcelains. Mullite and corundum are created during the sintering process, and porcelain is produced with a high glass phase content that prevents porosity but does not cause the aluminum oxide grain to melt.[5]

When the literature is examined, it becomes apparent that porcelain is typically employed for accident dosimetry, retrospective dosimetry, or dating.[6–16] Ancient porcelain samples are frequently TL-dated using the pre-dose effect 110°C TL peak of quartz,[6] a significant porcelain constituent. Pre-dose measurements of the 110°C and/or 230°C TL peaks, and additive dose measurement of 230°C TL peak are common techniques applied using porcelain for retrospective dosimetry.[17] Göksu et al.[18] reported that the pre-dose method for porcelain can also be inserted into the 230°C TL peak, which has the benefit of a longer half-life and higher linearity at absorbed doses than the 110°C TL peak. In addition, Adamiec et al.[15,19] recorded the TL released from the porcelain sample and observed the similar outcomes by the pre-dose method over the 110°C and 230°C TL peak and a straightforward additive dose method for the 230°C TL peak. There is a close relationship between the pre-dose behavior of porcelain and that of quartz, implying that the presence of quartz influences the observed TL. Regarding how the crystallinity of quartz affects TL emission, Topaksu et al.[20] reported that mineralogical formation, crystallinity index, and impurity content are the main parameters affecting the shape intensity of TL emission in hydrothermal and metamorphic quartz. The emission would primarily be related to inherent flaws such as oxygen vacancies, lattice flaws, hydroxyl flaws that act as precursors to non-bridging oxygen hole centers, substitutional point flaws, $[AlO_4]^\circ$ centers of substitutional Al^{3+}, and impurities that change the crystal structure.[20] Mullite, on the other hand, has been found as a probable active participant in the TL signal of porcelain.[21] Mullite[22] is one of the primary ingredients of porcelain as well, but existing methods for preparing porcelain samples for TL dating are unable to entirely separate quartz from mullite. According to research, TL signals from mullite may have an impact on the outcome of TL dating.[16] To minimize the inaccuracies in TL dating, knowledge of the specific luminescence characteristics of mullite is required. Adamiec,[19] on the other hand, found that mullite is unlikely to contribute to the 230°C TL peak of porcelain based on the shape of the TL glow curve of the porcelain, TL emission spectra, and pre-dose sensitivity. It was also discussed that mullite gives a wide range of TL emissions between 100°C and 400°C. Almost all prior porcelain investigations evaluated TL emission in the blue zone (usually 280–380 nm). However, Göksu et al.[14] discovered that the major TL emission was in two bands at 360 and 420 nm, with a third band at 640 nm. Oks et al.[13] investigated the TL properties of electrically insulating porcelain in order to develop better protocols for retrospective dosimetry. For this purpose, spatial, spectral, and kinetic measurements were made on various electrical insulators. In their study, they determined that 230°C TL emission at 620 nm is potentially useful for retrospective dosimetry of radiological events over the past few decades. Furthermore, Sfampa et al.[7] made a valuable contribution by evaluating newly created and in vitro aged porcelain samples, and the measurements were also used on in vivo aged samples that were taken from patients. All of the samples, they noted, have at least one peak that is noticeable for dosimetric purposes.

The goal of the current work is to assess the appropriateness of a well-characterized porcelain used as an electrical insulator for environmental applications as a radiation dosimeter by studying the TL of the material. The sample, which was examined using XRD, SEM-EDS, AAS, and FTIR, was subjected to various beta doses for this purpose in order to assess (i) its reusability, (ii) its fading, and (iii) its dose response to the beta radiation relying on the TL emission. Additionally, TL kinetic analyses using the maximum versus stopping temperature (T_M–T_s), initial rise (IR), and computerized glow curve deconvolution (CGCD) techniques were carried out to establish the trap parameters. Each of the evaluations was utilized on un-annealed and annealed porcelain samples for the comparison.

15512916, 0, Downloaded from https://ceramics.onlinelibrary.wiley.com/doi/10.1111/jace.19472 by Cukurova University, Wiley Online Library on [26/09/2023]. See the Terms and Conditions (https://onlinelibrary.wiley.com/terms-and-conditions) on Wiley Online Library for rules of use; OA articles are governed by the applicable Creative Commons License

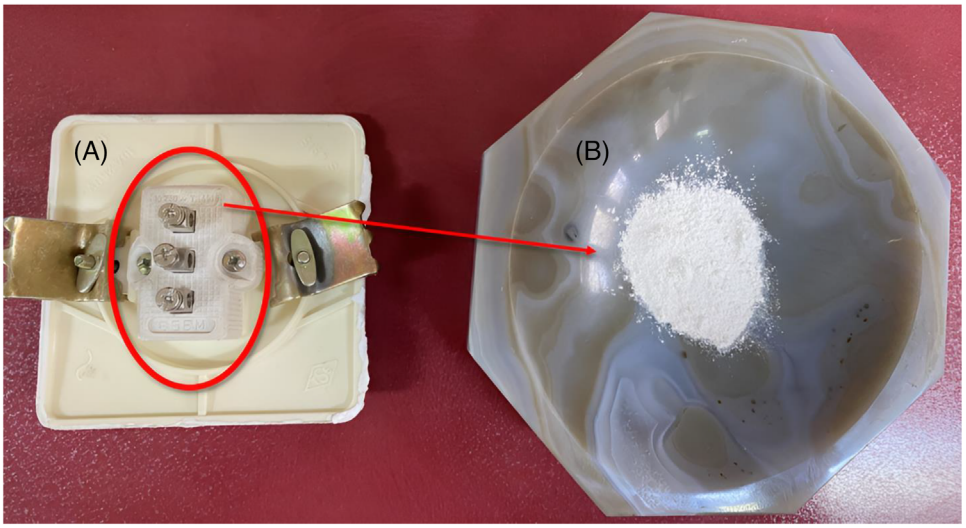

FIGURE 1 (A) Porcelain used in the ordinary switches; (B) fine powdered sample.

2 | MATERIALS AND METHODS

2.1 | Sample collection and preparation

Porcelain parts were removed from the ordinary switches that were changed during the renovation of the Faculty of Arts and Sciences, Çukurova University. The age of the samples did not exceed 40 years. These insulators are rectangular shaped, about 3.7 cm in length, 2.0 cm in width, and 1.5 thick, uncovered (Figure 1a). Using water that has been distilled, porcelain samples that were initially stored in an obscure location were cleaned. After the collected porcelain sample was broken into small pieces, the insulator was ground to a fine powder (Figure 1b) and homogenized by the Retsch RM 100 mortar grinder. The powdered porcelain samples were placed on alumina crucibles that can resist heat up to 1700°C in an electric furnace and fired between 500°C and 1200°C in increments of 100°C for an hour with a heating rate of 20°C/min. The powder samples were thereafter removed from the furnace and fast cooled to room temperature (RT) in air. For each TL measurement, 20 ± 3 mg powder samples were placed into the stainless steel disks ($\varnothing$ = 10.0 mm, h = 1.0 mm) using silicone oil.

2.2 | Structural, morphological, and elemental characterization

The composition of the phases and crystal structure of non-annealed and annealed porcelains were achieved using a PANalytical Empyrean X-ray diffractometer with Cu Kα radiation at 45 kV, 40 mA, and a wavelength of 0.15406 nm. At scanning increments of 0.01°, the 2θ values fell between the ranges of 10° and 90° with continuous scan type. The composition of the phases was evaluated by the matched reference cards.

FEI Quanta 650 field emission SEM was utilized to evaluate the surface morphology of non-annealed and annealed porcelain powder samples. In addition, EDS analysis was performed to achieve the composition of each sample. Each sample was given a 2 Å/s thick coat of gold during the procedure using a fine coating ion sputtering apparatus, Quorum-Q150R ES.

The porcelain sample was weighed as 100 mg and introduced to the digestion vessel together with H_3PO_4 (85%) as 5.0 mL, HCl (37%) as 3.0 mL, HF (40%) as 0.5 mL, and HNO_3 (65%) as 10 mL in order to detect the trace elements in porcelain. After giving the liquid a gentle swirl and waiting for around 10 min, the vessel was sealed. The combination was then broken down using a Berghof Speedwave Xpert microwave and examined using an AAS (PinAAcle 900T, Perkin Elmer) instrument.

A Jasco FT/IR-6700 FTIR spectrometer was used to perform FTIR in transmission (T) mode at mid-IR, with wavenumbers ranging from 400 to 4000 cm^{-1} (λ = 2.5–25 μm). A potassium bromide (KBr) matrix was used to disseminate the powder samples. IR spectra were captured with a 1 cm^{-1} resolution in an N_2 environment at RT.

2.3 | TL characterization

Following initial annealing tests, a powdered sample of each porcelain was generated for thorough TL characterization and kinetic parameter studies. Lexsyg Smart TL/OSL reader, an automated device, was used for whole TL study as it exposed non-annealed and annealed

15512916, 0, Downloaded from https://ceramics.onlinelibrary.wiley.com/doi/10.1111/jace.19472 by Cukurova University, Wiley Online Library on [26/09/2023]. See the Terms and Conditions (https://onlinelibrary.wiley.com/terms-and-conditions) on Wiley Online Library for rules of use; OA articles are governed by the applicable Creative Commons License

porcelain samples to a $^{90}Sr/^{90}Y$ beta source with an actual dose rate of 0.097 Gy/s and a maximum energy of 2.2 MeV. The reader has a photomultiplier tube (PMT) including UV–vis bi-alkaline cathode with an emission range of 300–650 nm. To utilize the most practical TL glow curves with the ideal TL intensity and the least amount of noise, various filter combinations were used. The TL reader has variable band-pass filter combinations, such as BSL-TL 365 nm (U340 + BP365/50 EX), IRSL-TL 410 nm (BG39 + HC414/46), IRSL-TL 565 nm (BG39 + HC575/25), and IRSL-TL wideband blue (BG39 + BG25 + KG3), which are placed between the PMT and the required sample. A linear heating rate of 2°C/s was utilized to generate TL glow curves for all of the samples from RT till 500°C using various band-pass filter combinations in the reader. To determine the dosimetric TL peak(s) of the non-annealed and annealed porcelain samples using equivalent measurement conditions, dose linearity, repeatability, storage period, and kinetic studies were used after choosing the most practical optical filter combination. After all, the background was subtracted from each initial TL reading before recording the net TL responses for each measurement.

3 | RESULTS AND DISCUSSION

3.1 | XRD analysis

Determining whether a material is crystalline or amorphous is the first step in any examination of the XRD results. If the material is amorphous, expansive diffuse areas of scatter rather than sharp diffraction peaks will make up the diffraction pattern. An extensive library of reference diffraction data is necessary for phase identification after crystalline phase(s) have been detected in a sample based on XRD data. The diffraction peaks of the non-annealed porcelain are shown in Figure 2. Phases of 898-004-2498 quartz (SiO_2) with hexagonal crystal system, 98-006-6445 mullite ($Al_{4.8}Si_{1.2}O_{9+x}$) with an orthorhombic crystal system, and 98-010-0452 sillimanite (Al_2SiO_5) with an orthorhombic crystal system were recorded in the XRD pattern of porcelain, as shown in Figure 2a.

Feldspar and kaolinite were not observed in XRD. This may be due to the fact that the XRD threshold does not allow the identification of components of the poly mineral samples at a rate lower than 3%–4%. Although not shown here, a certain amount of overlap with the tridymite phases was also obtained. The 2θ peaks at 20.8° and 26.6° correspond to (0 1 0) and the major (0 1 1) crystal lattice plane diffractions of quartz. Figure 2b shows the XRD patterns of all porcelain samples annealed between 500°C and 1200°C and a non-annealed one. The findings indicate that quartz is the main material present in all samples. The crystalline matrix form is generally found in all the samples. The annealing procedure did not alter the structure of the phosphor, according to the findings in Figure 2b.

3.2 | SEM-EDS analysis

Figure 3 displays SEM microstructure images at ×10,000 magnification of non-annealed and annealed porcelain samples at 500°C, 800°C, 1000°C, 1100°C, and 1200°C. Last three images were taken to see the effect of high-temperature annealing on the morphology of the porcelain material. As seen in Figure 3, SEM photographs of each sample showed irregular morphology. There are several unmelted quartz grains throughout the substance. The major portion of the images had an aggregated structure of both dark and light particles because atoms with greater mass backscatter electrons more vigorously than lighter atoms, which makes them seem somewhat brighter. An entire region of a chosen SEM image was used for the evaluation of the EDS analysis findings on the non-annealed sample in Figure 4. When the field measurement findings are analyzed, it is possible to observe the elemental values that correspond to the mineralogical composition of the porcelain samples. The XRD patterns and the EDS results from non-annealed and annealed samples, which are tabulated in inset of Figure 4, are in agreement. Furthermore, the presence of Na and K in Figure 4 indicates that, contrary to the XRD results, the porcelain sample has a high potential for small contents of alkali-rich feldspars that, as described by Correcher et al.,[23] could be used for dosimetric purposes.

3.3 | AAS analysis

By identifying the trace element(s) present in the porcelain sample, AAS analysis added to the body of knowledge used in this investigation to comprehend the composition of the material and luminescence process. The required wavelengths and the presence of the necessary elements were reported in ppm. Ten elements (Al, Pb, Ca, Co, Cu, Fe, Mg, Mn, Zn, and K) were evaluated by AAS, and their concentrations for non-annealed and annealed at 1100°C porcelain samples are shown in Table 1. A number of the elements found in porcelain may be TL killers (quenching), sensitizers, and activators. It is also possible that a particular impurity or defect is prevalent in a sample, yet does not directly affect the observed TL emission. However, Al is of great importance due to its contribution to the TL emission (Ref.[20] and references therein). Together, these imperfections have an impact that gives porcelain its distinctive TL output.

15512916, 0, Downloaded from https://ceramics.onlinelibrary.wiley.com/doi/10.1111/jace.19472 by Cukurova University, Wiley Online Library on [26/09/2023]. See the Terms and Conditions (https://onlinelibrary.wiley.com/terms-and-conditions) on Wiley Online Library for rules of use; OA articles are governed by the applicable Creative Commons License

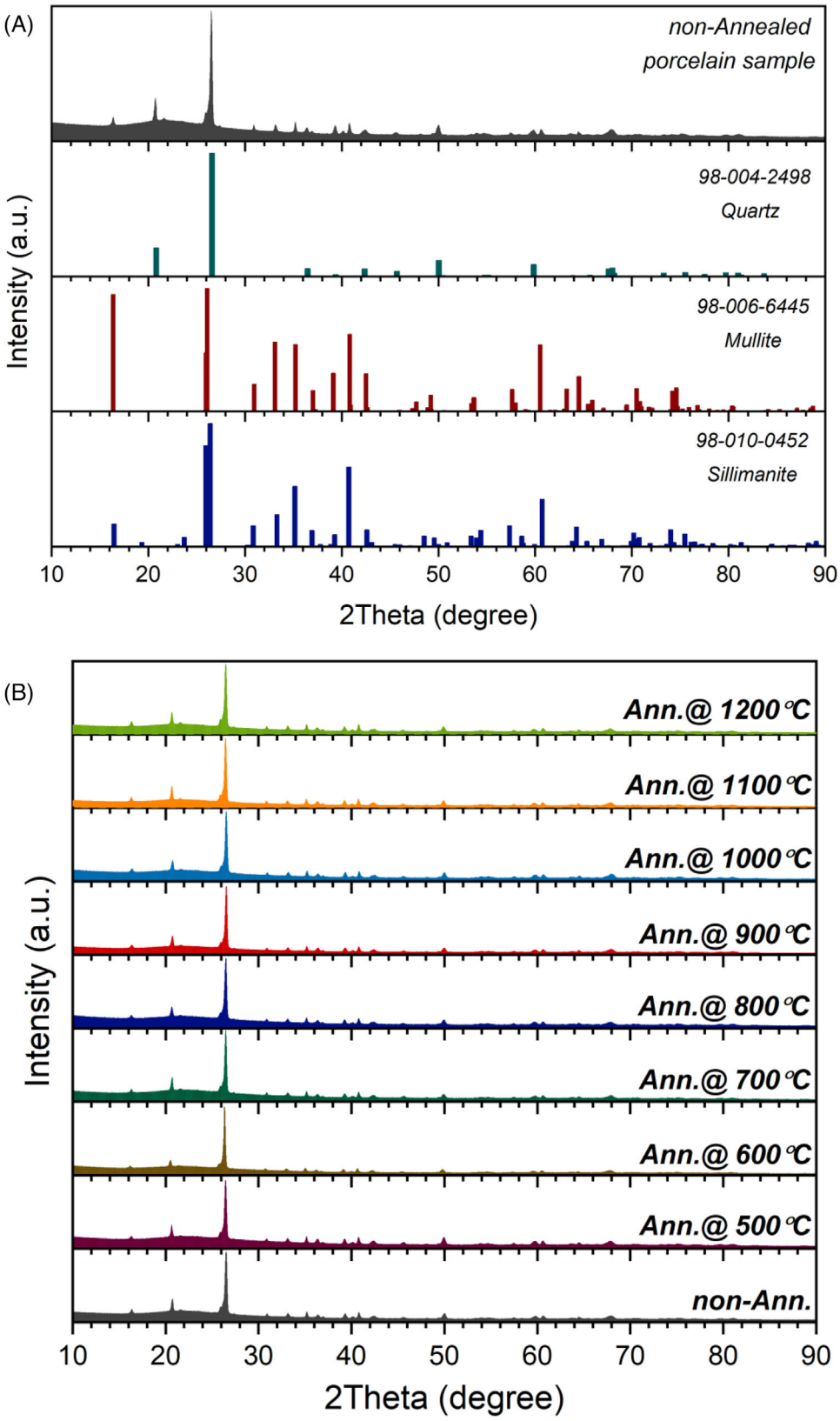

FIGURE 2 (A) X-ray diffraction (XRD) pattern of powdered non-annealed porcelain with the matched ref. cards; (B) patterns of non-annealed and annealed porcelains.

15512916, 0, Downloaded from https://ceramics.onlinelibrary.wiley.com/doi/10.1111/jace.19472 by Cukurova University, Wiley Online Library on [26/09/2023]. See the Terms and Conditions (https://onlinelibrary.wiley.com/terms-and-conditions) on Wiley Online Library for rules of use; OA articles are governed by the applicable Creative Commons License

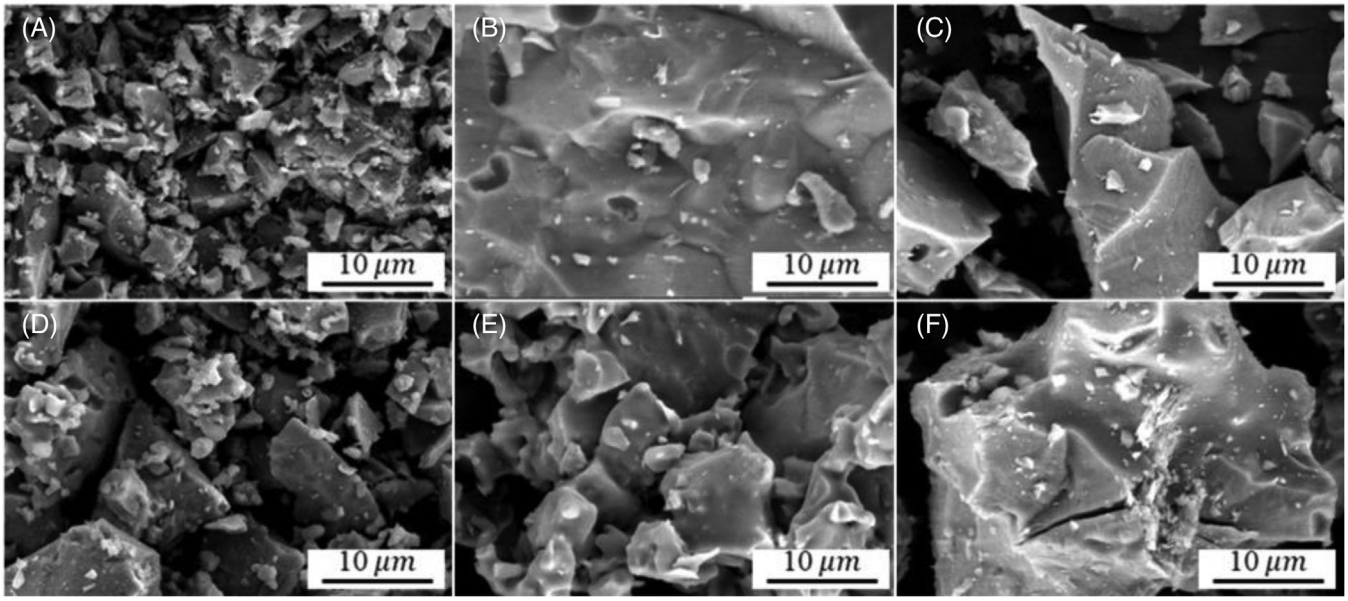

FIGURE 3 Scanning electron microscopy (SEM) images of porcelain for (A) non-annealed and (B–F) annealed samples at 500°C, 800°C, 1000°C, 1100°C, and 1200°C, respectively.

3.4 | FTIR analysis

The transmittance intensities of the non-annealed and annealed porcelain samples are depicted in Figure 5 along with a detailed representation of the transmittance peak intensities at wavenumbers between 400 and 4000 cm^{-1}. Stretching vibrations between hydrogen and several other atoms as well as a variety of double- and triple-bonded functional groups, such as carbonyls and allenes, frequently cause the formation of significant absorption bands in the range of 4000–1400 cm^{-1}.[4] The samples are slightly hygroscopic, but it would be challenging to locate them using FTIR analysis since the most important bands of water molecules (adsorbed on the surface of both annealed and non-annealed samples) have a low concentration. However, one can infer the presence of weak signals or even overlapped bands (at lower wavenumber) corresponding to the following: (i) asymmetric O–H stretching band (3300–3700 cm^{-1}), (ii) symmetric O–H stretching band (3100–3500 cm^{-1}), (iii) H–O–H angular bending band (1600–1700 cm^{-1}), and (iv) O–H deformation band (400–1500 cm^{-1}). Depending on the experimental setup and the resolution of the FTIR spectrometer, the location of these bands may partially change. In this regard, ionizing radiation may cause the radiolysis of the adsorbed water molecules, where the hydroxyl groups may be weakly linked to cations (Al^{3+}, Si^{4+}, etc.); these OH^- are released owing to the rise in the temperature (during the readout). When hydroxyl groups from water dissociation or hydro-peroxide breakdown are adsorbed on the surface of an insulator solid, the UV-green emission from the material is enhanced.[24] Figure 5 displays the IR spectra of the transmittance vibrational bonds of silicon in the wavenumber region of 400–1400 cm^{-1}. In order to define the unit of the Si–O–Si vibrational absorption features and specifically examine the phase separation and silicon crystallization of silica-based materials, the Si–O–Si IR spectra are frequently reported in this region.[25] Si–O vibrational bands that are rocking, bending and stretching can potentially be seen in the IR spectra of SiO_2 at wavelengths of 450, 800, and 1080 cm^{-1}, respectively.[26] Therefore, the strong bands nearly at 1079–1082 cm^{-1}, 794–796 cm^{-1}, and 455–459 cm^{-1} were associated with the asymmetric and symmetric stretching vibrations and bending vibrations of the Si–O–Si bond in both the samples. The absorption peak determined round 692–694 cm^{-1} could be attributed to the Si–O–Al vibrations.[27]

No changes in the spectral structure could be seen, as was observed. The sample underwent an intense thermal treatment, however, this had no effect on the chemical composition of the sample; no bonds were broken as a result of the heating. Examination of the transmission samples revealed that the forms of Si–O–Si bonds alter as a result of the annealing temperature, which ranges from 2 to 4 cm^{-1}. As the annealing temperature is raised, the band slowly moves to higher wavenumbers. It is assumed that this occurs as a result of the tighter bonding brought on by the densification of SiO_2.

15512916, 0, Downloaded from https://ceramics.onlinelibrary.wiley.com/doi/10.1111/jace.19472 by Cukurova University, Wiley Online Library on [26/09/2023]. See the Terms and Conditions (https://onlinelibrary.wiley.com/terms-and-conditions) on Wiley Online Library for rules of use; OA articles are governed by the applicable Creative Commons License

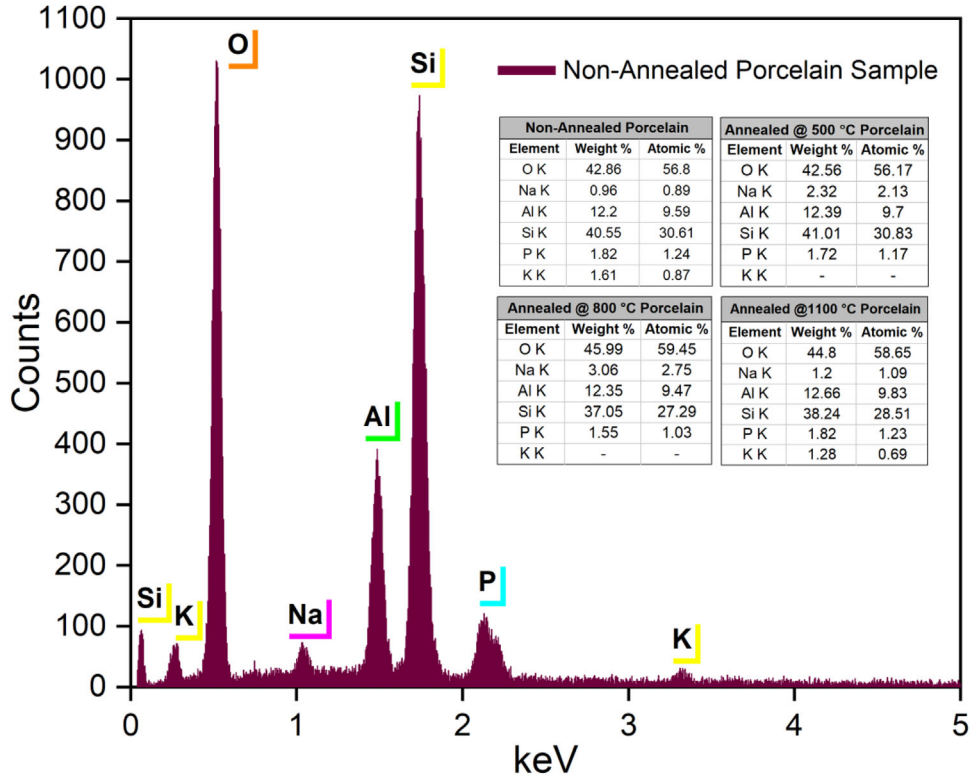

FIGURE 4 Energy dispersive X-ray spectroscopy (EDS) of non-annealed porcelain with the detailed ingredients of both non-annealed and annealed samples (inset).

TABLE 1 Concentrations of trace elements for non-annealed and annealed porcelain samples measured by atomic absorption spectrometry.

Trace element	Concentration (ppm)		Wavelength (Å)
	Non-annealed	Annealed (1100°C, 1 h)	
Al	13 903.743	10 587.523	3092.7
Pb	–	–	2833.1
Ca	1185.383	1253.786	4226.7
Co	–	–	2407.3
Cu	–	–	3247.5
Fe	3077.837	2834.646	2483.3
Mg	210.933	184.737	2852.1
Mn	–	–	2794.8
Zn	–	360.388	2138.6
K	11 212.121	10 669.291	7664.9

3.5 | TL dosimetric analysis

A spectrum of the TL emission with which the detection protocol (PMT and accompanying optical filters) can effectively interact is one of the most advantageous features of a dosimetric substance. Therefore, it is crucial to monitor changes in the ability of the filters to transmit light between the planchets and the PMT. To choose the best detection filter combination for the TL investigation, all sample types were analyzed using each filter combination. For each, the $^{90}Sr/^{90}Y$ beta source delivered a dose of 0.5 Gy to porcelain material (Figure 6). The optical filter is critical for removing the thermal radiation background. Selecting the best band-pass filter requires consideration of several criteria. To allow appropriate emission light to pass, it is necessary to suppress the black-body signal. Furthermore, when utilizing a material for dosimetric purposes, the presence of non-shallow traps that cause TL peaks at substantially higher temperatures is essential. As a consequence, a filter (or combination) that has no background effect, can pass a high-intensity TL signal, and has peaks on the higher temperature side is chosen.

The findings using IRSL TL 565 nm filter combination were outstanding when the obtained TL glow curves of non-annealed porcelain were evaluated (Figure 6). Furthermore, the glow curves produced with the BSL TL 365 nm and IRSL TL 410 nm combinations of the filters have the exact identical structure as those achieved with the IRSL TL 565 nm filter combination, yet with significantly lower intensity. When utilizing the wideband blue filter combination illustrated in Figure 6, a distinct glow curve was formed when compared to the other filters, and the existence of peak at roughly 380°C was noticed in

15512916, 0, Downloaded from https://ceramics.onlinelibrary.wiley.com/doi/10.1111/jace.19472 by Cukurova University, Wiley Online Library on [26/09/2023]. See the Terms and Conditions (https://onlinelibrary.wiley.com/terms-and-conditions) on Wiley Online Library for rules of use; OA articles are governed by the applicable Creative Commons License

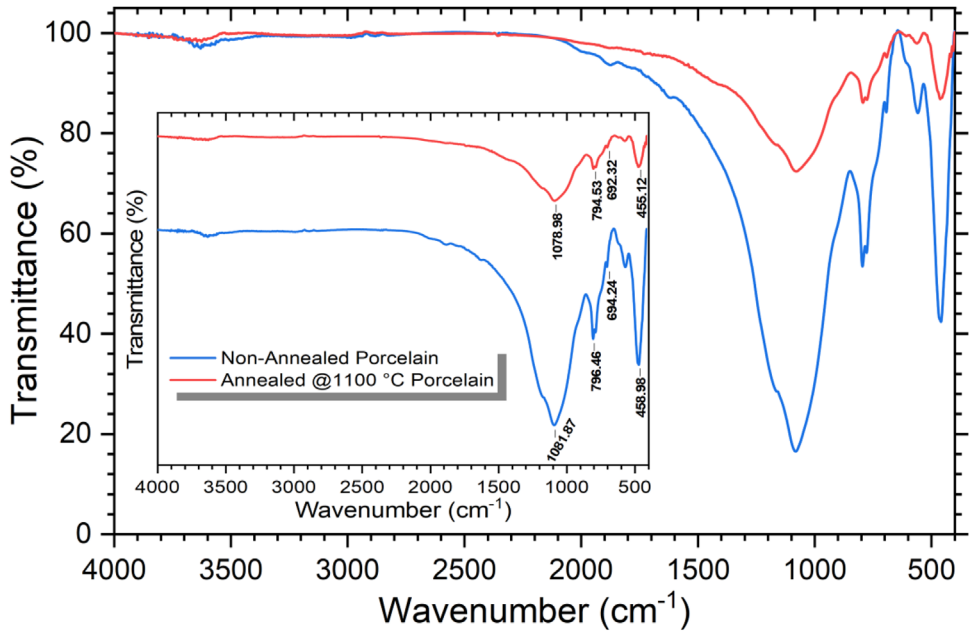

FIGURE 5 Fourier transform infrared spectroscopy (FTIR) spectra of non-annealed and annealed porcelain samples.

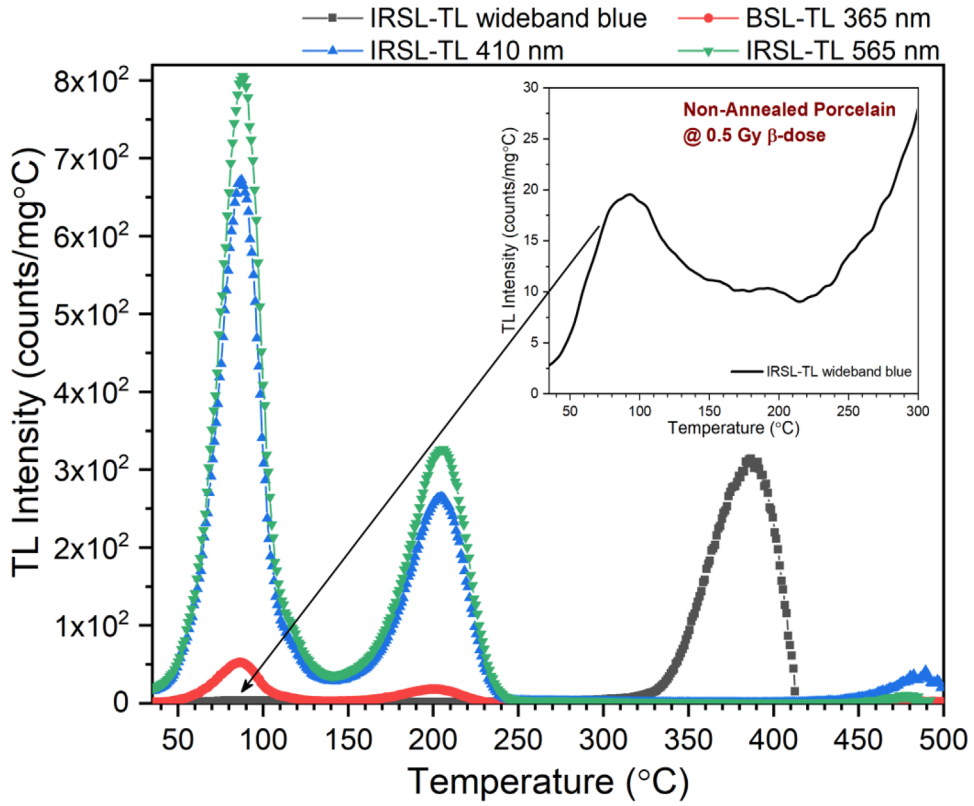

FIGURE 6 Thermoluminescence (TL) glow curves of non-annealed porcelain sample after 0.5 Gy beta irradiation obtained by various band-pass filter combinations. Inset: glow curve obtained by using wideband blue filter combination.

15512916, 0, Downloaded from https://ceramics.onlinelibrary.wiley.com/doi/10.1111/jace.19472 by Cukurova University, Wiley Online Library on [26/09/2023]. See the Terms and Conditions (https://onlinelibrary.wiley.com/terms-and-conditions) on Wiley Online Library for rules of use; OA articles are governed by the applicable Creative Commons License

addition to the ~90°C and ~200°C TL peaks. However, when determining the most adequate filter combination for this investigation, the presence and intensity of the peaks in the dosimetric temperature region were taken into account. Therefore, IRSL-TL 565 nm band-pass filter combination was chosen for the further TL analysis of the porcelain.

A heat treatment procedure, commonly referred to as annealing, must be carried out in order to get a thermoluminescent material ready for usage in dosimetric applications. The TL samples are heated to a specific temperature during this procedure, which is subsequently performed in an oven. The samples are then maintained at this temperature for a specific amount of time before being cooled to RT.[28] Any earlier residual irradiation impact that was meant to stay stored in the crystal after the reading was removed using this procedure. The main goal of this heat treatment is to restore the initial structure of the trap-recombination center, which was established following the initialization process.

A novel TL material must first undergo an annealing study with two primary objectives before it can be utilized for the first time. (i) To stabilize the trap structure by finding a favorable annealing temperature and time combination; (ii) to create the least intrinsic background and to achieve the best TL response repeatability.[29] The created TL glow curves for annealed and non-annealed porcelains consistently demonstrate an identical structure with no discernible change in peak position or form. Increasing annealing temperature caused a decrease in the first apparent peak intensity and an increase in the second one. As shown, less stable shallower trapping centers are the reason for the apparent peak in the low-temperature region of the TL glow curve configuration of porcelain. To choose the appropriate annealing temperature, the dosimetric temperature region is therefore given priority. In the line with the purpose of the study, the effect of annealing had been examined and the most proper annealing temperature was decided on TL analyses as 1100°C (Figure 7). Even though the annealing time data are not provided here, 1 h was chosen as the best treatment time. Further characterizations over both non-annealed and 1100°C annealed samples were made in the framework.

One of the most important properties that a TL material must have in order to find its place in a dosimetry application is its reusability. The TLD material should exhibit a similar TL response after each irradiation and heating cycle. To determine the reusability of non-annealed and 1100°C annealed porcelain samples, 10 cycles of 0.5 Gy beta dose exposure and heating from RT to 500°C were performed.

Each cycle was performed for three sets of measurements and the variation in the TL peak areas of the glow curves recorded as a result of each reading is shown in Figure 8a,b. The peak areas of the TL glow curves obtained after each cycle were calculated and normalized to the peak area of the glow curve obtained after the first TL reading. The amount of deviation observed as a result of three measurements for each cycle, the deviation from the mean value, and the deviation from the first value were analyzed. After 10 cycles, it can be seen that the peak area variation for both non-annealed (max. 3%) and 1100°C annealed (max. 2%) samples is within the 5% confidence interval (CI) (seen in Figure 8a,b). When the deviation values are analyzed as the deviation of three measurements, deviation from the mean value and the first value, they are 4%–5%, max. 0.6% and max. 1.1% for the non-annealed samples and 2%–3%, max. 0.5% and max. 0.8% for the samples annealed at 1100°C, respectively. In light of these results, it can be said that in general, both sample types have reusability, although it is clear that the usability of the porcelain sample annealed at 1100°C is better.

It is desirable that the TL signals of the dosimetric peaks of materials that are candidates for use as dosimeters do not fade out in a short time. Therefore, to determine the time-dependent fading behavior of the TL emissions of porcelain samples, the samples were exposed to a beta dose of 0.5 Gy and kept in a dark environment at RT for certain periods of time. The short-term (maximum 7 days) fading behavior was investigated by the variation in the TL intensities of the glow peaks for non-annealed and 1100°C annealed samples (Figure 9a,b). Accordingly, it was observed that the TL emission of the low-temperature peak at about 90°C, given as the first maximum, completely faded within 7 days for both sample types, while the TL emission of the dosimetric peak at 200°C, given as the second maximum, decreased by 4.9% for non-annealed samples (Figure 9a, inset) and 10.2% for annealed samples (Figure 9b, inset) during this period. These results for both sample types show, as expected, that the TL emissions of the dosimetric peaks do not fade rapidly without external influences.

The prior knowledge of kinetic order b and exact number of glow peaks in the glow curve are important for the determination of E and s in the TL studies.[30] Therefore, in this study, the dose–response method was employed for an idea about the kinetic order, b, of each individual glow peak of non-annealed and annealed porcelain sample treated at 1100°C. Both non-annealed and annealed porcelain samples were exposed to various doses ranging from 0.1 to 30 Gy, and the TL glow curves were recorded using a heating rate of 2°C/s to investigate the influence of dose on peak positions. According to TL theory, changes in the heating rate are expected to result in variations in the peak temperature of the glow peak. Hence, under constant heating rate, the peak temperature

15512916, 0, Downloaded from https://ceramics.onlinelibrary.wiley.com/doi/10.1111/jace.19472 by Cukurova University, Wiley Online Library on [26/09/2023]. See the Terms and Conditions (https://onlinelibrary.wiley.com/terms-and-conditions) on Wiley Online Library for rules of use; OA articles are governed by the applicable Creative Commons License

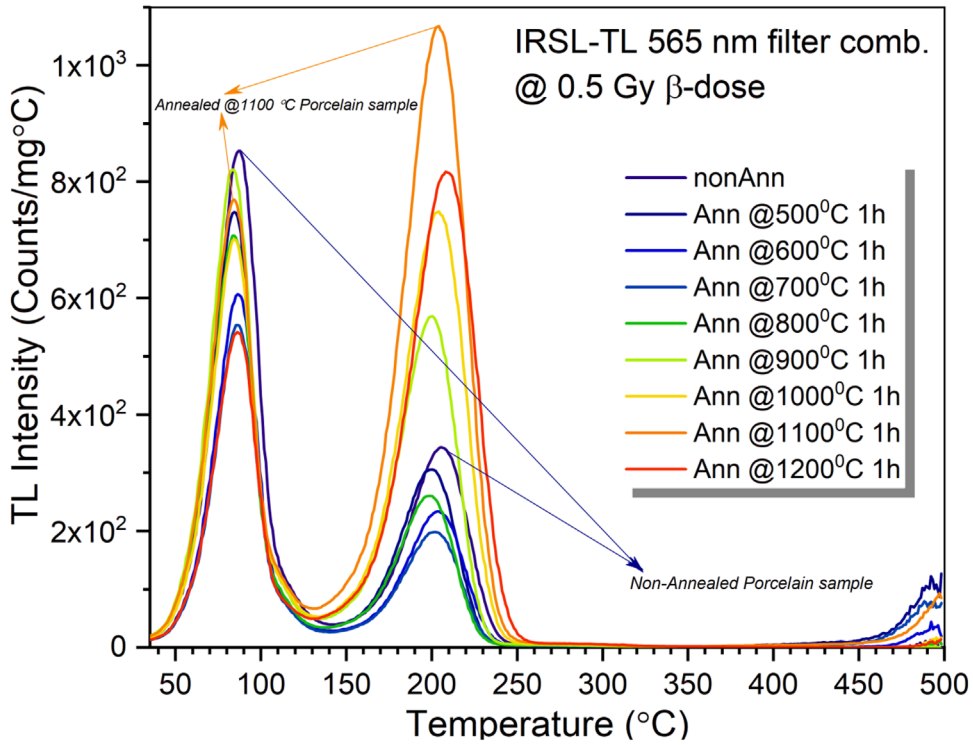

FIGURE 7 Thermoluminescence (TL) glow curve of powdered non-annealed and annealed porcelain samples.

remains unaffected by other experimental parameters in the case of first-order kinetics. However, for general order kinetics and doses below trap saturation points, the peak temperatures tend to shift toward lower temperature regions as the dose level increases. Figure 10a,b shows the TL glow curves for non-annealed and annealed porcelain samples. As seen Figure 10a,b, the dose–response experimental observations clearly show that it consists of two main maxima, centered at about 87°C and 207°C, and also there is a slight shoulder at approximately 120°C. The shape of the TL glow curves for both non-annealed and annealed porcelain samples does not significantly change with increasing dose level (Figure 10a,b). Since the recorded position of the glow peaks is not affected by the increase in radiation dose amount, one can say that the TL glow curves likely exhibit first-order kinetics. Furthermore, the increase in TL glow curve intensity with the deposition of beta irradiation in the porcelain can be attributed to an increase in the number of radiative centers.

Figure 10c illustrates the TL response as a function of the dose for the non-annealed and annealed porcelain samples in the studied range. All obtained experimental data from dose–response measurements were plotted on log–log scale. It is clearly seen from Figure 10c that the dose responses of non-annealed porcelain are linear between 0.1 and 2.5 Gy with a slope of 0.95 and a correlation coefficient of 0.99 after it starts to follow sublinearity up to 20 Gy and then starts to saturate. On the other hand, annealed porcelain samples exhibit linear dose responses between 0.1 and 3 Gy with a slope of 0.96 and a correlation coefficient of 0.99 after it starts to follow sublinearity up to 20 Gy and then starts to saturate. Additionally, it was determined that the minimum detectable dose (MDD) for non-annealed and annealed porcelain was 0.4 and 0.5 mGy, respectively. The MDD demonstrates its dependability rather than limiting its usage to low dose irradiation investigations. The environment and the elements that the TL reader identified as the lowest dosage recognized with a reasonable degree of confidence influence the MDD quantity.[31] The requirements are three times the TL value at zero dose's standard deviation (σ_{BG}).

3.6 | TL kinetics analysis

T_M–T_S and IR techniques were used to evaluate the kinetic parameters of non-annealed and annealed porcelain. In addition, the CGCD approach was used to determine if the monitored glow curve had overlapping TL peaks. One of the various methodologies for separating overlapping TL peaks is to preheat to a stopping temperature (T_S) before obtaining the TL glow curve. To achieve this, a beta-exposed sample is heated at a linear rate to T_S, which corresponds to a place on the low-temperature tail of the first TL peak. The quickly cooled sample is subsequently

15512916, 0, Downloaded from https://ceramics.onlinelibrary.wiley.com/doi/10.1111/jace.19472 by Cukurova University, Wiley Online Library on [26/09/2023]. See the Terms and Conditions (https://onlinelibrary.wiley.com/terms-and-conditions) on Wiley Online Library for rules of use; OA articles are governed by the applicable Creative Commons License

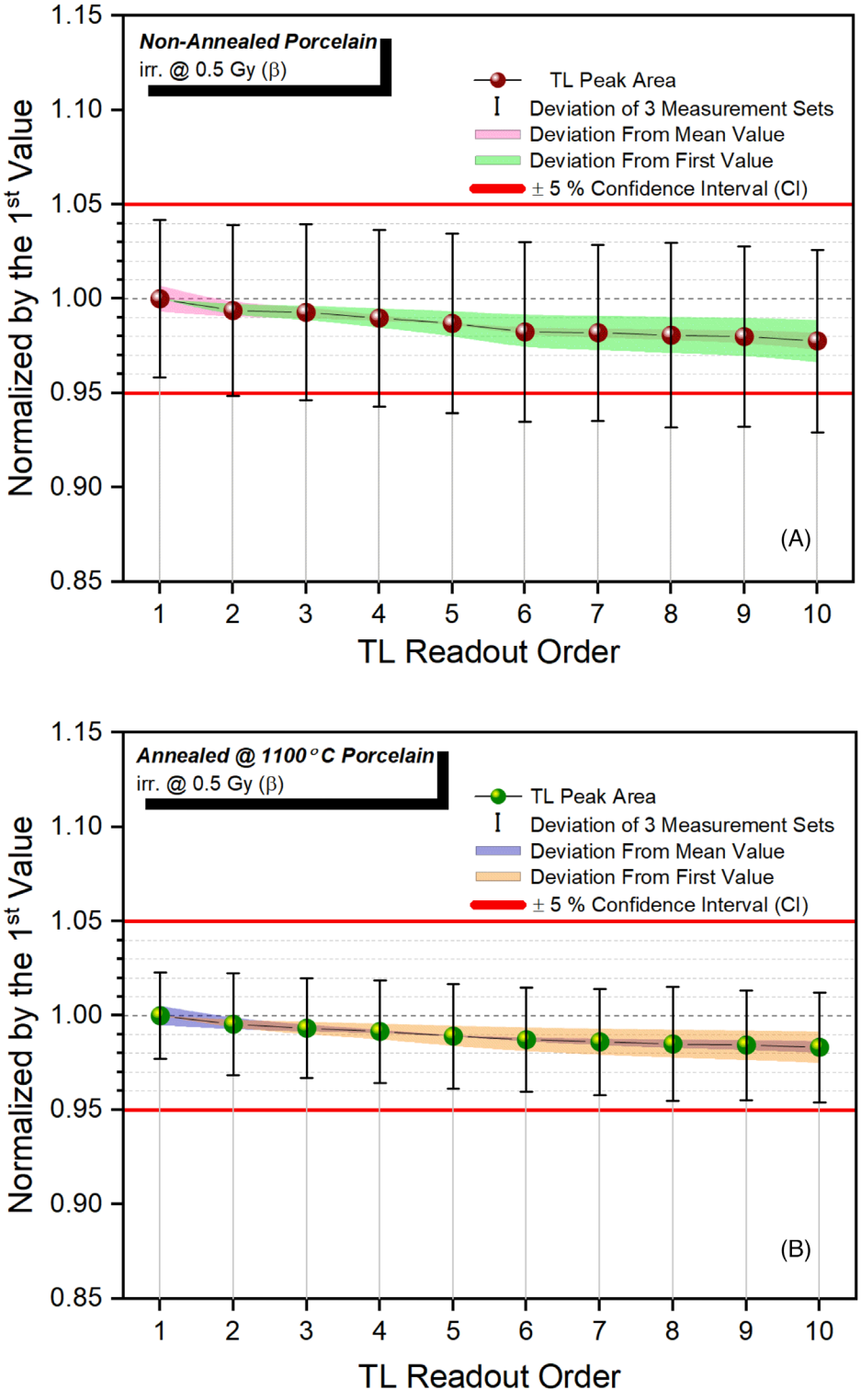

FIGURE 8 Changes in the peak areas of the thermoluminescence (TL) glow curves of (A) non-annealed and (B) annealed at 1100°C porcelain samples in 10 cycles.

heated at an identical heating rate to acquire the rest of the TL glow curve, and the location of the first maximum temperature (T_M) is determined. The technique is repeated for newly irradiated samples with varied T_s that are raised by a slight increment (in the range of 2°C–5°C). This approach and the T_M–T_s method are commonly employed for determining the quantity and likely locations of overlapping TL peaks. In general, the T_M–T_s plot may be shown in two ways: as a "staircase" form or as a "continuous line" with a slope of one.[32]

15512916, 0, Downloaded from https://ceramics.onlinelibrary.wiley.com/doi/10.1111/jace.19472 by Cukurova University, Wiley Online Library on [26/09/2023]. See the Terms and Conditions (https://onlinelibrary.wiley.com/terms-and-conditions) on Wiley Online Library for rules of use; OA articles are governed by the applicable Creative Commons License

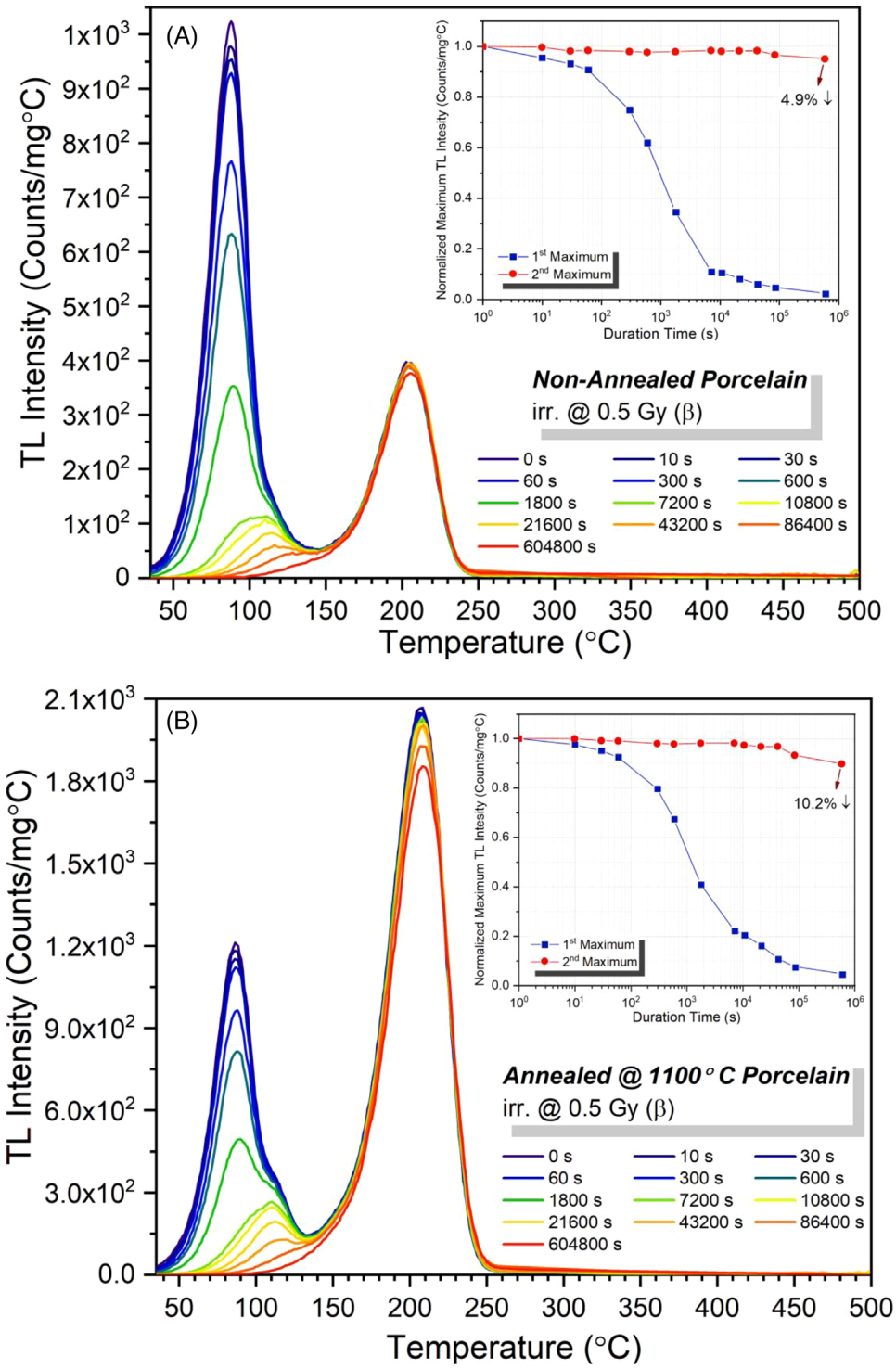

FIGURE 9 Change in thermoluminescence (TL) glow curves of (A) non-annealed and (B) annealed at 1100°C porcelain samples against the storage time. The inset figures show the rate of change of both maxima.

Each porcelain sample was initially given a 0.5 Gy beta dose before being heated to a certain T_S. The TL glow curve was then created using a constant heating rate of 2°C/s. This cycle was repeated under the same circumstances, but with T_S values at increments of 5°C from 30°C to 225°C (Figure 11). The T_M–T_S approach is commonly utilized for determining the number and position of overlapping TL peaks. As a result, T_M versus T_S graphs for the TL glow curve data of each porcelain sample were obtained and are shown in Figure 12a. If a TL glow curve has many clearly separated first-order TL peaks, the T_M–T_S curve has a distinct "staircase" structure with discrete flat areas. When a

15512916, 0, Downloaded from https://ceramics.onlinelibrary.wiley.com/doi/10.1111/jace.19472 by Cukurova University, Wiley Online Library on [26/09/2023]. See the Terms and Conditions (https://onlinelibrary.wiley.com/terms-and-conditions) on Wiley Online Library for rules of use; OA articles are governed by the applicable Creative Commons License

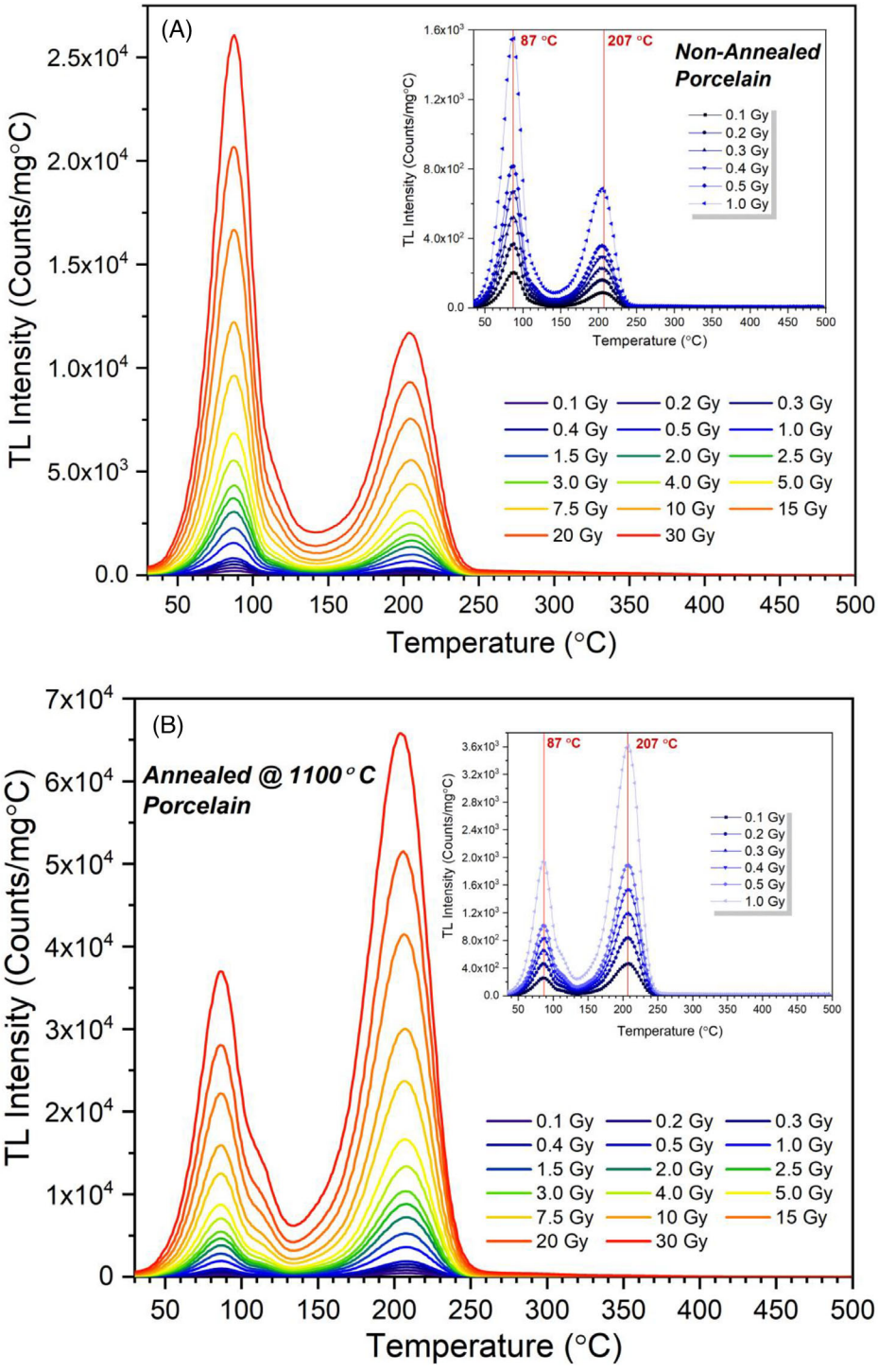

FIGURE 10 (A and B) Dose dependence of non-annealed and annealed porcelain samples exposed to beta doses in the range of 0.1–30 Gy at 2°C/s. The inset shows the plot for integrated thermoluminescence (TL) peak intensity versus dose in the range of 0.1–1.0 Gy. (C) Linearity plot of unannealed and annealed porcelain samples.

glow curve has more closely overlapping peaks, the curve becomes smoother, and the T_M representing the flat portions can only be used as a signal of the positions of each individual peak. It should be noted that a separate individual peak can appear in a T_M–T_s plot regardless of whether the zone is flat or curved. This technique only draws attention to the TL glow curve's most prominent peaks.[32] The exact location of the visible maximum is denoted by the symbol T_M. Both non-annealed and annealed porcelains produced identical T_M–T_s plots, as shown in Figure 12a, and it was found that the glow curves had at least three overlapping peaks. As seen, possible separated TL peaks

15512916, 0, Downloaded from https://ceramics.onlinelibrary.wiley.com/doi/10.1111/jace.19472 by Cukurova University, Wiley Online Library on [26/09/2023]. See the Terms and Conditions (https://onlinelibrary.wiley.com/terms-and-conditions) on Wiley Online Library for rules of use; OA articles are governed by the applicable Creative Commons License

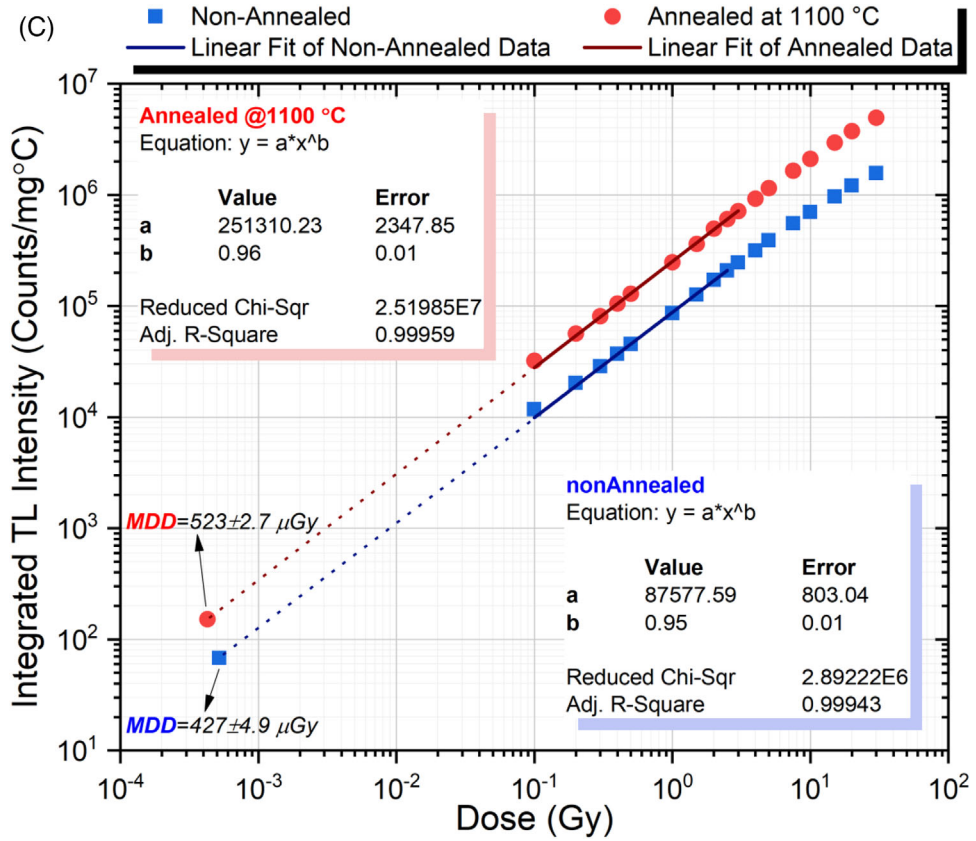

FIGURE 10 Continued

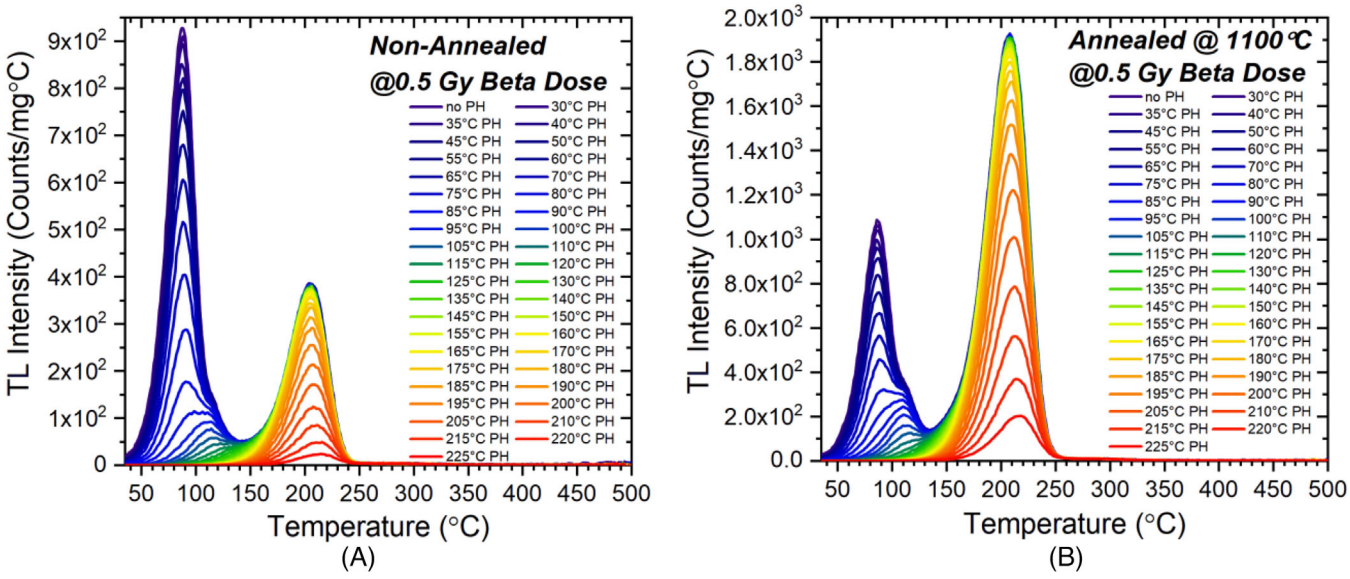

FIGURE 11 Thermoluminescence (TL) glow curves versus T_s for (A) non-annealed and (B) annealed porcelain.

may be located at around 87°C–88°C, 111°C–114°C, and 206°C–208°C.

The IR approach, which is a very reliable way to get trap parameters, was also used to investigate the activation energy, E, of each sample by employing T_M–T_s analysis. Therefore, each glow curve acquired following the T_M–T_s analysis was subjected to this procedure. By applying the IR approach to each TL peak at a distinct T_s, the mean activation energies of these energy levels were calculated. Figure 12b shows the calculated E values plotted

15512916, 0, Downloaded from https://ceramics.onlinelibrary.wiley.com/doi/10.1111/jace.19472 by Cukurova University, Wiley Online Library on [26/09/2023]. See the Terms and Conditions (https://onlinelibrary.wiley.com/terms-and-conditions) on Wiley Online Library for rules of use; OA articles are governed by the applicable Creative Commons License

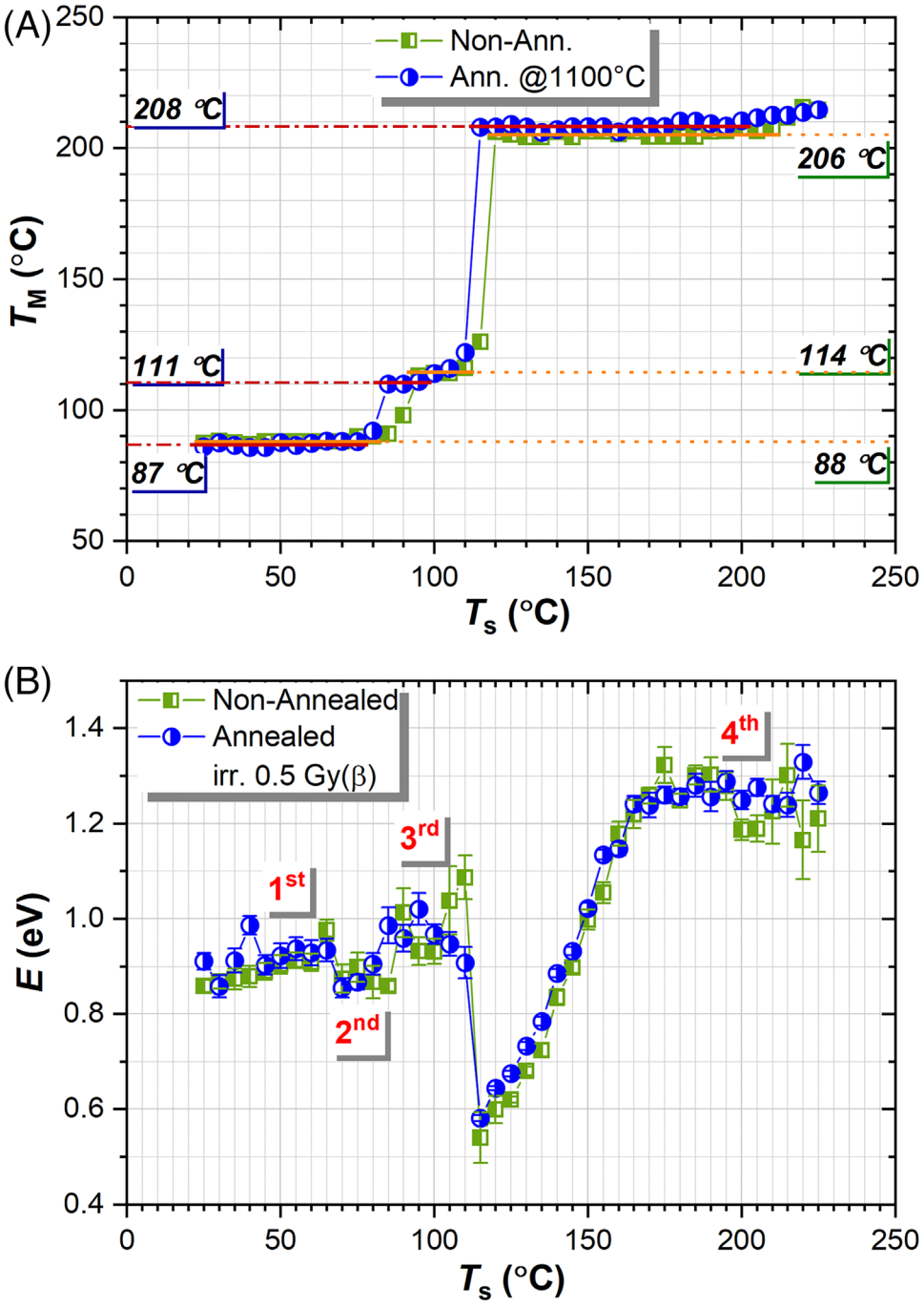

FIGURE 12 (A) T_M–T_s and (B) E–T_s plots for each porcelain sample.

against the applied T_s. As can be observed in Figure 12b, each porcelain sample contains four trap levels with activation energies of around 0.90, 0.85, 1.00, and 1.30 eV, supporting the conclusion of Figure 12a. This demonstrates that whereas the peak in the higher temperature region is practically one unique TL peak, the maximum in the low-temperature region comprises of almost three overlapping TL peaks. However, in line with this knowledge, the most accurate information will be obtained as a result of decomposition below.

Decomposing the TL glow peak and obtaining the kinetic parameters of the non-annealed and annealed porcelains are done using the CGCD technique. This strategy is repeatable because by varying the kinetic parameters we obtain the greatest match between the theoretical and experimental curves using the general order kinetic model. The results of the T_M–T_s investigation are very important in this context. As a result of the knowledge gathered regarding the number and location of probable TL peaks, the decomposition analysis can be concluded

15512916, 0, Downloaded from https://ceramics.onlinelibrary.wiley.com/doi/10.1111/jace.19472 by Cukurova University, Wiley Online Library on [26/09/2023]. See the Terms and Conditions (https://onlinelibrary.wiley.com/terms-and-conditions) on Wiley Online Library for rules of use; OA articles are governed by the applicable Creative Commons License

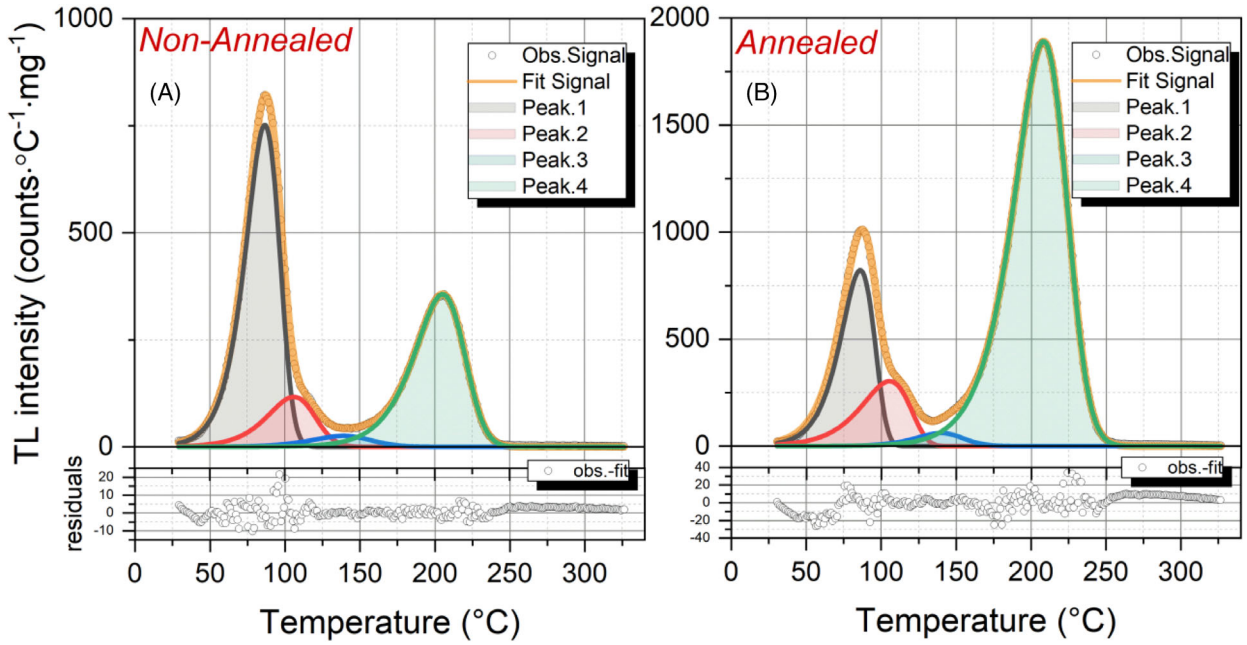

FIGURE 13 Computerized glow curve deconvolution (CGCD) results using a general order empirical expression (r.o.i. of each fit is up to 350°C) (A) non-annealed; (B) annealed.

more quickly and accurately. The open-source R package "tgcd,"[33] which employs the Fortran language for programming to accelerate calculations and the R language to improve adaptability was used to help with the deconvolution inquiry. This package allows for the employment of complex optimization techniques.[34] The experimental TL glow curve of the sample with 0.5 Gy beta exposure at a heating rate of 2°C/s was adequately fitted with four TL peaks, as shown by the CGCD plot and decomposed TL glow peaks in Figure 13. The following equation was used to operate the CGCD technique.[35]

$$I\ (T) = I_{\mathrm{M}} \exp\left(\frac{E}{kT_{\mathrm{M}}^2}(T - T_{\mathrm{M}})\right) \times \left[\frac{1}{b} + \frac{b-1}{b}\exp\left(\frac{E}{kT_{\mathrm{M}}^2}(T - T_{\mathrm{M}})\right)\right]^{-(b/b-1)} \quad (1)$$

Here, I_{M} stands for maximum intensity, s for frequency factor, k for Boltzmann constant, E for activation energy, and b for kinetic order ($1 \leq b \leq 2$). Four unique energy levels were reached in the ranges of 1.02–1.29 eV and 1.08–1.32 eV for the annealed and non-annealed porcelain samples, respectively. Considering figure of merit values of 1.69% and 1.75%, respectively, it can be demonstrated that the deconvolution findings of porcelain samples provide a trustworthy evaluation of the trap parameters.

Additionally, in the semi-logarithmic graph (Figure 14), the separated peaks for the annealed and unannealed porcelain samples are shown and contrasted by overlapping. As it was emphasized before, the main structure of the glow curve of porcelain remained unchanged after annealing at 1100°C, and it was observed that there was a significant increase in the number of trapped electrons in the higher temperature region. The symmetry factors, frequency factors, and activation energies of the four peaks are listed in Table 2. Between experimental and theoretical data with the E levels and T_{M} values, there is substantial concordance. It is also seen that the results are in agreement with the results obtained by T_{M}–T_{s} and IR methods. Furthermore, lifetimes (τ) of the TL light peaks provide a strong justification for examining the use of TL materials for dosimetry. Chen[36] demonstrated that $\mu = 0.42$ and 0.52 describe the first-order ($b = 1$) peak and the second-order ($b = 2$) peak, respectively. All of the separated peaks, with the exception of the third peak, have first-order kinetic characteristics, as can be shown by examining the symmetry factors. The circumstance stated in the dosage response and the existence of the step structure in the T_{M}–T_{s} plot are both present in this instance. The peak at 140°C, which could not be seen on the T_{M}–T_{s} plot, was found to be in accordance with the general order kinetics.

4 | CONCLUSION

In the current study, the potential of porcelain, an electrical insulator, was examined as a radiation dosimeter for use in environmental applications. The XRD pattern of

15512916, 0, Downloaded from https://ceramics.onlinelibrary.wiley.com/doi/10.1111/jace.19472 by Cukurova University, Wiley Online Library on [26/09/2023]. See the Terms and Conditions (https://onlinelibrary.wiley.com/terms-and-conditions) on Wiley Online Library for rules of use; OA articles are governed by the applicable Creative Commons License

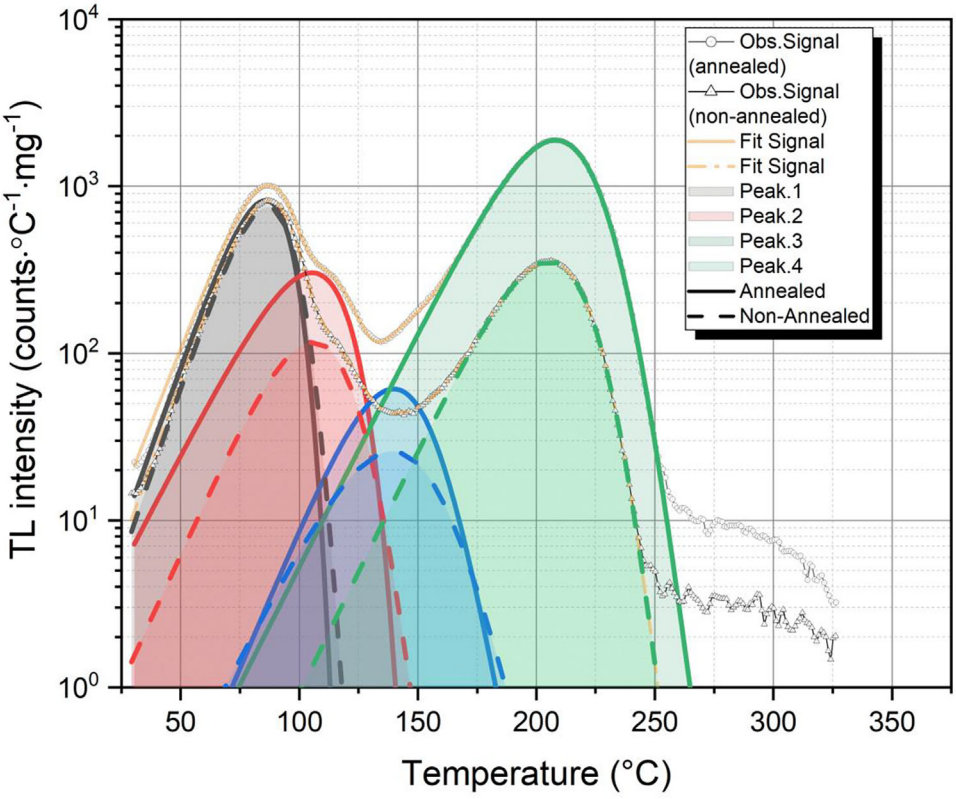

FIGURE 14 Semi-logarithmic and merged computerized glow curve deconvolution (CGCD) results of annealed and non-annealed thermoluminescence (TL) glow curve spectra. Solid lines and dashed lines are for annealed and no-annealed samples, respectively.

TABLE 2 Kinetic parameters obtained by the computerized glow curve deconvolution (CGCD) analyses of the annealed porcelain and non-annealed porcelain samples (figure of merit [FOM]: 1.69% and 1.75%, respectively).

	E (eV)	T_M (°C)	T_{M1} (°C)	T_{M2} (°C)	μ	b	s (s^{-1})	τ (year)
Annealed sample								
First peak	1.02	86	70	97	0.42	1.04	3.83×10^{13}	1.44×10^{-4}
Second peak	0.78	105	82	121	0.40	1.01	3.06×10^{9}	1.59×10^{-4}
Third peak	1.14	140	119	157	0.46	1.42	1.23×10^{13}	4.80×10^{-2}
Fourth peak	1.29	208	184	226	0.42	1.23	4.18×10^{12}	4.85×10^{1}
Non-annealed sample								
First peak	1.08	87	71	98	0.44	1.15	2.25×10^{14}	2.54×10^{-4}
Second peak	0.89	106	84	122	0.43	1.24	9.53×10^{10}	3.68×10^{-4}
Third peak	0.92	139	114	161	0.45	1.45	2.22×10^{10}	5.08×10^{-3}
Fourth peak	1.32	205	182	222	0.43	1.2	1.06×10^{13}	6.14×10^{1}

porcelain was matched with the phases of quartz (SiO_2), mullite ($Al_{4.8}Si_{1.2}O_{9+x}$), and sillimanite (Al_2SiO_5). The results showed that quartz is the primary component in each sample. All of the samples consistently turned out to be in the crystalline matrix type and the structure was unaltered by the annealing process between 500°C and 1200°C. In addition to the EDS analysis, trace elements were evaluated by AAS and the presence of Al, Ca, Fe, Mg, Zn, and K was recorded. A number of the elements found in porcelain are TL killers, sensitizers, and activators. Together, these imperfections have an impact that gives porcelain its distinctive TL output. The asymmetric, symmetric stretching vibrations, and bending vibrations of the Si–O–Si link in both samples were related to the strong bands roughly at 1079–1082 cm^{-1}, 794–796 cm^{-1}, and 455–459 cm^{-1} in the FTIR data, which also confirm the XRD results. The Si–O–Al vibrations may be responsible for the absorption peak seen between 692 and 694 cm^{-1}.

15512916, 0, Downloaded from https://ceramics.onlinelibrary.wiley.com/doi/10.1111/jace.19472 by Cukurova University, Wiley Online Library on [26/09/2023]. See the Terms and Conditions (https://onlinelibrary.wiley.com/terms-and-conditions) on Wiley Online Library for rules of use; OA articles are governed by the applicable Creative Commons License

When the acquired TL glow curves of non-annealed porcelain were analyzed, the results obtained employing the IRSL TL 565 nm band-pass filter combination were exceptional. After being exposed to beta radiation, samples that had been annealed at 1100°C and non-annealed ones were analyzed using TL glow curves. The samples show two broad maxima that are well defined and are situated at 87°C and 207°C. Additionally, there was a slight shoulder at about 120°C. For non-annealed and annealed porcelain, respectively, the obtained glow curves show a linear behavior between 0.1–2.5 Gy and 0.1–3 Gy. Additionally, it is proposed that, with a 5% CI, both non-annealed and annealed porcelain are suitable materials for dosimetric applications. According to the length of storage in the dark environment, it was also found that the time-dependent change in the intensity of the high-temperature peak was rather small. Additionally, utilizing T_M–T_s data, the trapping parameters of the IR technique were examined. The outcomes were contrasted with those obtained from glow curves that had been deconvoluted. Each procedure was discovered to be consistent with the outcomes based on the findings attained. The results of the comprehensive examinations showed that the sample was appropriate for possible TL dosimetry usage.

ACKNOWLEDGMENTS

This work was supported by the Research Fund of Cukurova University, Turkey (project number: FBA-2021-14293).

ORCID

Ziyafer Gizem Portakal-Uçar https://orcid.org/0000-0002-3827-423X
Mehmet Oglakci https://orcid.org/0000-0003-1096-5087

REFERENCES

1. Furetta C. Handbook of thermoluminescence. Singapore: Word Scientific; 2003. https://doi.org/10.1142/5167
2. Khamidova LG, Ivannikova AI, Kondrashov AE, Tikounov DD, Skvortsov VG, Stepanenko VF, et al. Possibility of using porcelain samples of high-voltage line insulators for radiation dose reconstruction by EPR spectroscopy. Appl Radiat Isot. 2001;55:843–48. https://doi.org/10.1016/S0969-8043(01)00147-6
3. Amigo JM, Serranoa FJ, Kojdecki MA, Bastida J, Esteve V, Reventos MM, et al. X-ray diffraction micro structure analysis of mullite, quartz and corundum in porcelain insulators. J Eur Ceram Soc. 2005;25:1479–86. https://doi.org/10.1016/j.jeurceramsoc.2004.05.019
4. Shahrokh Abadi MH, Delbari A, Fakoor Z, Baedi J. Effects of annealing temperature on infrared spectra of SiO_2 extracted from rice husk. J Ceram Sci Tech. 2015;06:41–46. https://doi.org/10.4416/JCST2014-00028
5. Amigo JM, Clausell JV, Esteve V, Delgado JM, Reventos MM, Ochando LE, et al. X-ray powder diffraction phase analysis and thermomechanical properties of silica and alumina porcelains. J Eur Ceram Soc. 2004;24:75–81. https://doi.org/10.1016/S0955-2219(03)00119-5
6. Bailiff IK. Pre-dose dating. In: Goksu HY, Oberhofer M, Regulla D, editors. Scientific dating methods. Eurocourses: advanced scientific techniques. Vol. 1. CEC, Dordrecht: Kluwer Academic Publishers; 1991; 155-74.
7. Sfampa IK, Malletzidou L, Pandoleon P, Kitis G. Thermoluminescence measurements of in-vitro and in-vivo aged porcelain. Radiat Meas. 2019;125:7–14. https://doi.org/10.1016/j.radmeas.2019.04.017
8. Wang WD. Study and progress of the thermoluminescence dating of the ancient pottery and porcelain. Sci China Series E: Technol Sci. 2009;52:1613–40. https://doi.org/10.1007/s11431-009-0106-4
9. Stoneham D, Green TH, Voice E. Porcelain slices as a stable thermoluminescence dosemeter up to 500°C. Radiat Prot Dosim. 1986;17:251–54. https://doi.org/10.1093/oxfordjournals.rpd.a079817
10. Bøtter-Jensen L, Markey BG, Poolton NRJ, Jungner H. Luminescence properties of porcelain ceramics relevant to retrospective radiation dosimetry. Radiat Prot Dosim. 1996;65:369–72. https://doi.org/10.1093/oxfordjournals.rpd.a031663
11. Kim MJ, Lee YJ, Lee JI, Kim JL, Hong DG. Fading test using the SAAD-POSL method for retrospective accidental dosimetry of building materials. Radiat Phys Chem. 2015;116:373–76. https://doi.org/10.1016/j.radphyschem.2015.04.002
12. Ramzaev V, Göksu HY. Cumulative dose assessment using thermoluminescence properties of porcelain isolators as evidence of a severe radiation accident in the Republic of Sakha (Yakutia), Russia, 1978. Health Phys. 2006;91:263–69. https://doi.org/10.1097/01.HP.0000215837.68118.d3
13. Oks H, Spooner NA, Smith BW, Prescott JR, Creighton DF, McCulloch I, et al. Assessment of thermoluminescence peaks in porcelain for use in retrospective dosimetry. Radiat Meas. 2011;46:1873–77. https://doi.org/10.1016/j.radmeas.2011.06.067
14. Göksu HY, Wieser A, Stoneham D, Bailiff IK, Figel M. EPR, OSL, TL and spectral studies of porcelain. Appl Radiat Isot. 1996;47(11/12):1369–74. https://doi.org/10.1016/S0969-8043(96)00137-6
15. Adamiec G, Stoneham D, Göksu Y. Accident dose estimation using porcelain. A comparison between different thermoluminescence methods. Radiat Meas. 1997;27:389–92. https://doi.org/10.1016/S1350-4487(96)00119-9
16. Leung PL, Yang B. Thermoluminescence and X-ray diffraction studies on sliced ancient porcelain samples. Nucl Instr Meth B. 1999;155:452–58. https://doi.org/10.1016/S0168-583X(99)00482-6
17. Aitken MJ. Thermoluminescence dating. Academic Press; 1985. p. 271.
18. Göksu HY, Stoneham D, Bailiff IK, Adamiec G. A new technique in retrospective TL dosimetry: pre-dose effect in the 230°C TL glow peak of porcelain. Appl Radiat Isot. 1998;49:99–104. https://doi.org/10.1016/S0969-8043(97)00218-2
19. Adamiec G. Aspects of pre-dose and other luminescence phenomena in quartz absorbed dose estimation. Ph.D. Thesis. UK: University of Oxford; 2000.
20. Topaksu M, Correcher V, Garcia-Guinea J, Topak Y, Göksu HY. Comparison of thermoluminescence (TL) and cathodoluminescence (ESEM-CL) properties between hydrothermal and

15512916, 0, Downloaded from https://ceramics.onlinelibrary.wiley.com/doi/10.1111/jace.19472 by Cukurova University, Wiley Online Library on [26/09/2023]. See the Terms and Conditions (https://onlinelibrary.wiley.com/terms-and-conditions) on Wiley Online Library for rules of use; OA articles are governed by the applicable Creative Commons License

metamorphic quartzes. Appl Radiat Isotopes. 2012;70:946–51. http://doi.org/10.1016/j.apradiso.2012.03.017

21. Stoneham D. Porcelain dating. In: Hackens T, Mejdahl V, Bowman SGE, Wintle AG, Aitken MJ, editors. PACT 9. 1983. p. 227–39; Roskilde (Denmark): Risoe National Laboratory; 3. Specialist seminar on TL and ESR dating. Elsinore (Denmark); 26–31 July 1982.
22. Griffen DT. Silicate crystal chemistry. New York, Oxford: Oxford University Press; 1992. https://doi.org/10.1180/minmag.1996.060.398.18
23. Correcher V, Gómez-Ros JM, Delgado A. The use of albite as a dosemeter in accident dose reconstruction. Radiat Prot Dosim. 1999;84(1–4):547–49. http://doi.org/10.1093/oxfordjournals.rpd.a032795
24. Garcia-Guinea J, Correcher V, Can N, Garrido F, Townsend PD. Cathodoluminescence spectra recorded from surfaces of solids with hydrous molecules. J Electron Spectrosc Relat Phenom. 2018;227:1–8. https://doi.org/10.1016/j.elspec.2018.05.008
25. Nobuyoshi K. Device applications of silicon nanocrystals and nanostructures. New York: Springer Science & Business Media; 2009. https://doi.org/10.1007/978-0-387-78689-6
26. Moore C, Perova TS, Kennedy BJ, Berwick K, Shaganov II, Moore RA. Study of structure and quality of different silicon oxides using FTIR and Raman microscopy. Proceedings of SPIE, Opto-Ireland 2002: Optics and Photonics Technologies and Applications, Galway, Ireland, 5 September. Thomas J Glynn. 4876. 2003. p. 1247–56. https://doi.org/10.1117/12.464024
27. Čiuladienė A, Luckutė A, Kiuberis J, Kareiva A. Investigation of the chemical composition of red pigments and binding media. Chemija. 2018;29:243–56. https://doi.org/10.6001/chemija.v29i4.3840
28. Zhang Y, Jin S, Yang Y, Chunsheng Y. Annealing effects on the phase and microstructure transformations of nanocrystalline $(ZrO_2)_{1-x}(Sc_2O_3)_x$ ($x = 0.02$–0.16) thin films deposited by sol–gel method. Solid State Commun. 2002;122:439–44. https://doi.org/10.1016/S0038-1098(02)00152-7
29. Rivera T. Synthesis and thermoluminescent characterization of ceramics materials. In: Sikalidis C, editor. Advances in ceramics—synthesis and characterization, processing and specific applications. InTech; 2011. https://doi.org/10.5772/17423
30. Kirsh Y. Kinetic analysis of thermoluminescence. Phys Stat Sol A. 1992;129:15–148. https://doi.org/10.1002/pssa.2211290102
31. Del Sol Fernández S, Garcia-Salcedo R, Guzmán Mendoza J, Sánchez-Guzmán D, Ramírez Rodríguez G, Gaona E, et al. Thermoluminescent characteristics of LiF:Mg, Cu, P and $CaSO_4$:Dy for low dose measurement. Appl Radiat Isotopes. 2016;111:50–55. https://doi.org/10.1016/j.apradiso.2016.02.011
32. McKeever SWS. On the analysis of complex thermoluminescence glow-curves resolution into individual peaks. Phys Status Solidi. 1980;62:331–40. https://doi.org/10.1002/pssa.2210620139
33. Peng J, Dong ZB, Han FQ. tgcd: an R package for analyzing thermoluminescence glow curves. SoftwareX. 2016;5:112–20. https://doi.org/10.1016/j.softx.2016.06.001
34. Peng J, Kitis G, Sadek AM, Karsu Asal EC, Li Z. Thermoluminescence glow-curve deconvolution using analytical expressions: a unified presentation. Appl Radiat Isot. 2021;168:109440. https://doi.org/10.1016/j.apradiso.2020.109440
35. Gomez-Ros JM, Kitis G. Computerised glow curve deconvolution using general and mixed order kinetics. Radiat Prot Dosim. 2002;101:47–52. https://doi.org/10.1093/oxfordjournals.rpd.a006029
36. Chen R. On the calculation of activation energies and frequency factors from glow curves. J Appl Phys. 1969;40:570–85. https://doi.org/10.1063/1.1657437

How to cite this article: Portakal-Uçar ZG, Akça-Özalp S, Oglakci M, Barad A, Topaksu M. Assessment of structural and thermoluminescence characteristics of porcelain used as an electrical insulator. J Am Ceram Soc. 2023;1–19. https://doi.org/10.1111/jace.19472

15512916, 0, Downloaded from https://ceramics.onlinelibrary.wiley.com/doi/10.1111/jace.19472 by Cukurova University, Wiley Online Library on [26/09/2023]. See the Terms and Conditions (https://onlinelibrary.wiley.com/terms-and-conditions) on Wiley Online Library for rules of use; OA articles are governed by the applicable Creative Commons License